



Electric Field Stimulation for the Functional Assessment of Isolated Dorsal Root Ganglion Neuron Excitability

IAN M. BERKE¹,^{ORCID} TOM M. MCGRATH,¹ J. JORDAN STIVERS,²
CHANG GUI,¹ MARCOS N. BARCELLONA,¹ MATTHEW G. GAYOSO,¹
SIMON Y. TANG,^{2,3} YU-QING CAO,⁴ MUNISH C. GUPTA,³ and LORI A. SETTON^{1,2,3}

¹Department of Biomedical Engineering, Washington University in St. Louis, One Brookings Drive, Campus Box 1097, St. Louis, MO 63130, USA; ²Department of Orthopaedic Surgery, Washington University School of Medicine, St. Louis, MO 63110, USA; ³Musculoskeletal Research Center, Washington University School of Medicine, St. Louis, MO 63110, USA; and ⁴Department of Anesthesiology, Washington University School of Medicine, St. Louis, MO 63110, USA

(Received 26 August 2020; accepted 5 January 2021)

Associate Editor Rebecca Willits oversaw the review of this article.

Abstract—Genetically encoded calcium indicators have proven useful for characterizing dorsal root ganglion neuron excitability *in vivo*. Challenges persist in achieving high spatial–temporal resolutions *in vivo*, however, due to deep tissue imaging and motion artifacts that may be limiting technical factors in obtaining measurements. Here we report an *ex vivo* imaging method, using a peripheral neuron-specific Advillin-GCaMP mouse line and electric field stimulation of dorsal root ganglion tissues, to assess the sensitivity of neurons *en bloc*. The described method rapidly characterizes Ca^{2+} activity in hundreds of dorsal root ganglion neurons (221 ± 64 per dorsal root ganglion) with minimal perturbation to the *in situ* soma environment. We further validate the method for use as a drug screening platform with the voltage-gated sodium channel inhibitor, tetrodotoxin. Drug treatment led to decreased evoked Ca^{2+} activity; half-maximal response voltage (EV_{50}) increased from 13.4 V in untreated tissues to 21.2, 23.3, 51.5 ($p < 0.05$), and 60.6 V ($p < 0.05$) at 0.01, 0.1, 1, and 10 μM doses, respectively. This technique may help improve an understanding of neural signaling while retaining tissue structural organization and serves as a tool for the rapid *ex vivo* recording and assessment of neural activity.

Keywords—Calcium imaging, Drug screening, GCaMP, GECI, Nervous system, High content imaging.

INTRODUCTION

The functional assessment of cellular neurophysiology has traditionally relied on manual patch clamping or single unit recordings.³⁷ While these approaches remain the gold standard for understanding the electrophysiological basis of ion channel dynamics and action potential propagation, these approaches are limited due to their challenging technical methods and low-throughput.² When paired with calcium- or voltage-sensitive fluorescent indicators, optical imaging allows for the simultaneous capture of cellular signaling in diverse cell populations.¹³ Additionally, the development of genetically encoded calcium indicators (GECIs) allows for the spatiotemporal control of cell-type-specific indicator expression without the need for exogenous dye loading.³ Because calcium flux is a surrogate trailing measure of action potential propagation, GECIs have given investigators the freedom to study *in vivo* and *in vitro* neural signaling dynamics without the need for invasive patch clamping or exogenous dye loading.^{5,7,21}

The use of GECIs expressed in brain tissues has transformed the imaging of neuronal activity in living and awake mice, and found application to studies of neurovascular injury, neurodegenerative disease, and cancer.¹² GECIs have also found application to studies of the dorsal root ganglion (DRG) to study *in vivo* neuronal excitability in response to sensory stimuli.^{4,7,24,39} More recent studies have reported on novel methods for simultaneous electric field stimulation

Address correspondence to Lori A. Setton, Department of Biomedical Engineering, Washington University in St. Louis, One Brookings Drive, Campus Box 1097, St. Louis, MO 63130, USA. Electronic mail: setton@wustl.edu

Ian M. Berke and Tom M. McGrath have contributed equally to this work.

(EFS) with optical measures of GECI-expressing neurons bringing the disciplines of electrophysiology and optical imaging together in living and freely-behaving mice.^{15,34,35} While *in vivo* function in response to EFS remains the gold standard of quantifying neuronal excitability, there may be value in characterizing DRG neuron function *ex vivo* for drug screening or where deep tissue imaging and motion artifacts due to respiration may be limiting technical factors in obtaining measurements.¹

Gemes and co-workers have previously reported an imaging-based approach to assess electrically stimulated Ca^{2+} flux within isolated DRG tissues following intracellular micro-pipette injection of Fura-2.¹⁰ This injection approach was chosen as dye diffusion into the dense DRG tissue was unsuccessful in preliminary work. While insightful, intracellular micro-pipette injection reduced the throughput of their method as only tens of neurons could be assessed within individual DRG tissues. The use of GECIs extends this interest in isolated DRG tissues and improves assay throughput by providing robust and cell-type-specific Ca^{2+} indicator expression, thus, increasing the number of neurons that can be assessed within the DRG.

Here we describe the development of an EFS-mediated cellular imaging method using GECIs and spinning-disk confocal microscopy for the direct interrogation of calcium signaling dynamics in acutely isolated DRG tissues. The described method allows for the rapid and simultaneous characterization of functional excitability in hundreds of sensory neurons. Using this technique, we show an ability to detect dose-dependent excitability changes in *en bloc* DRG neurons in the presence of a voltage-gated sodium channel inhibitor. The described technique shows potential for the study of pharmacologically-induced alterations to large and heterogeneous neural populations without the need for dramatic perturbation to the DRG neurons' native microenvironment.

MATERIALS AND METHODS

Animal Model

All procedures were performed with approval of the Washington University in St. Louis Institutional Animal Care and Use Committee. Transgenic Advillin-CreERT2 (Cre/+, Stock No: 032027, The Jackson Laboratory, Bar Harbor, ME) mice were crossed with STOP-GCaMP6s (+/−, Stock No: 028866, The Jackson Laboratory) mice.^{3,20} Cre-positive mice received three consecutive doses of tamoxifen (i.p., daily,

75 mg/kg, Sigma-Aldrich, St Louis, MO) to induce GCaMP6s expression in Advillin expressing neurons (Figs. 1a and 1b). GCaMP6s was chosen for its high signal to noise ratio and slower temporal dynamics which enable its use in widefield, spinning-disk confocal, imaging. Three weeks following tamoxifen dosing, mice were utilized for electric field stimulation (EFS) experiments. Mice were maintained on a 12-h light–dark cycle with access to food and water *ad libitum*.

Dorsal Root Ganglion (DRG) Isolation

Mice were deeply anesthetized under isoflurane (3% inhalation, 2 L/min oxygen, $n = 6$, 16–20 weeks). A transcardial perfusion was performed with artificial cerebrospinal fluid (aCSF, 124 mM NaCl, 5 mM KCl, 20 mM HEPES, 10 mM D-glucose, 1.3 mM MgCl_2 , 1.5 mM CaCl_2 , 26 mM NaHCO_3 , 1.25 mM NaH_2PO_4)²³ after which the DRG tissues were isolated via a dorsal approach.⁹ Following a midline dorsal incision, paraspinal musculature, connective tissue, and fat were carefully removed with micro-dissection scissors to reveal the dorsal bony elements of the spine. Micro-rongeurs were then used to perform a multi-level laminectomy to expose the spinal cord, which was gently repositioned to expose the DRGs at each spinal level. Fine forceps were used to grasp the distal nerve root and gently remove the DRG from the neuroforamen, and spring scissors were used to carefully cut the nerve roots proximal and distal to the DRG. Isolated DRGs were then incubated in aCSF and used for EFS experiments within 8 h of isolation. All experiments were conducted with DRGs from thoracic level 13 through lumbar level 5.

Electric Field Stimulation (EFS)

Isolated DRGs were placed in the center of a recording chamber (RC-RC49MFSH, Warner Instruments, Hamden, CT), secured by a nylon mesh, and perfused with aCSF (2 mL/min) (Fig. 1c). Two parallel, linear platinum electrodes connected to a pulse generator (Grass SD9, Natus Neuro, Warwick, RI) were inserted at opposite ends of the recording chamber and DRGs were stimulated with bipolar square pulse waves (1 ms, 10 Hz, 1 s on/29 s off) at voltage amplitudes of 5–100 V (bath impedance 0.48 Ω at 10 Hz, Fig. 1d); these EFS parameters were chosen for their ability to evoke robust evoked Ca^{2+} transients within isolated DRG tissues as have been reported previously.^{5,7,8,10,16,19} The geometry of the recording chamber ensured the generation of a uniform electric

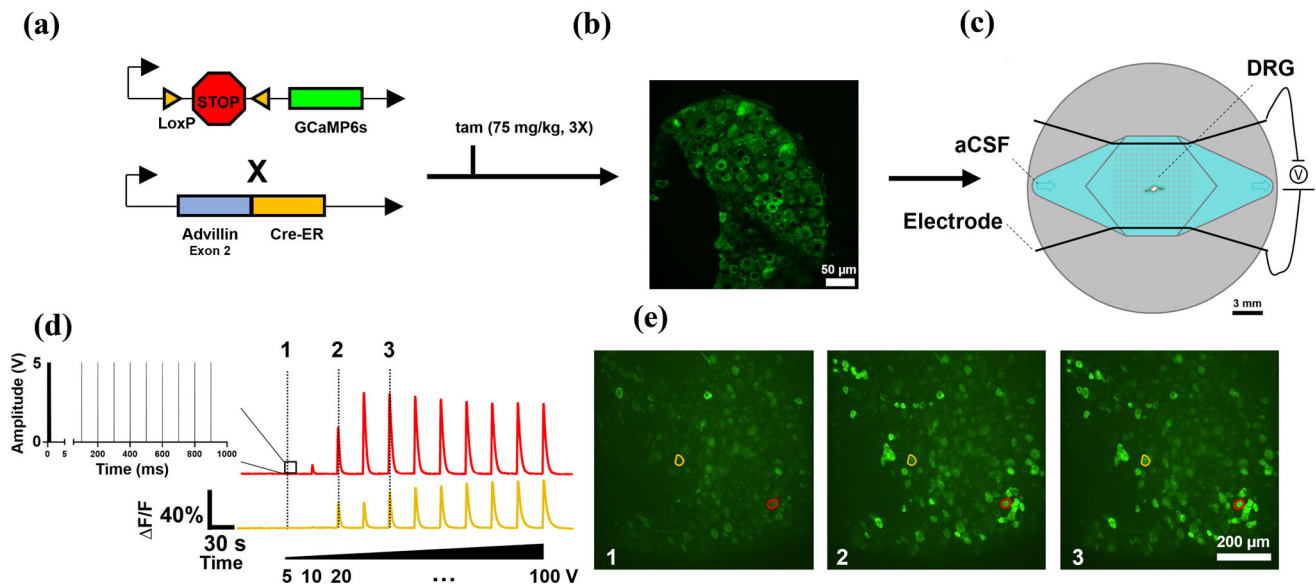


FIGURE 1. Experimental design. (a) Sensory neuron-specific expression of GCaMP6s was attained by crossing STOP-GCaMP6s (+/-) and Advillin-CreERT2 (Cre/+) mice. (b) Robust GCaMP expression in DRG neurons (scale bar = 50 μm) was observed 3 weeks following tamoxifen (tam, 75 mg/kg, i.p., 3 \times) dosing. (c) Isolated DRG tissues were placed within an EFS recording chamber beneath a nylon mesh and were continuously perfused with fresh artificial cerebrospinal fluid (aCSF, 2 mL/min). (d) Representative cellular traces of the normalized GCaMP fluorescence ($\Delta F/F$) and corresponding images show a rise in $\Delta F/F$ (e), with increasing voltage amplitudes (5–100 V). The inset depicts the applied excitatory pulse train that was used at each voltage (10 Hz, 1 ms pulse width); frames corresponding to each numbered peak are shown with color-coded cellular regions of interest (scale bar = 200 μm).

field between electrodes.¹⁰ Isolated DRG tissues were imaged (Plan Apo λ 10X, 0.45 NA, 4 mm WD) to collect GCaMP6s fluorescence (488/525 nm, ex/em, 10 Hz, 16 bit) upon an inverted spinning-disk confocal microscope (1220 \times 1220 px, 793 \times 793 micron field of view, Ti2-CSU-X1, Nikon Instruments, JPN) (Fig. 1e). Time series recordings at a single imaging plane (\sim 20 μm from tissue basal surface, 2.5 μm z-thickness) were acquired. Single recordings were completed in 6 min; DRGs (n = 13 tissues from 3 mice) were allowed to recover within the recording chamber for 5 min followed by repeated exposure to EFS in order to evaluate the repeatability of response and to confirm the viability of tested neurons.

Tetrodotoxin Inhibition

To test the ability of the described EFS imaging technique to be used for drug screening in isolated DRG tissues, the potent voltage-gated sodium channel (VGSC) inhibitor tetrodotoxin (TTX, Tocris, Minneapolis, MN) was used as described here.²⁵ DRGs (n = 5 tissues from 3 mice) underwent one voltage sweep (5–100 V) as described, followed by incubation with increasing concentrations of TTX (5 min incubation, 0.01–10 μM), and a repeat of the EFS voltage sweep protocol was performed.

Data Analysis

Following stimulation of DRGs in the EFS chamber, digital images of DRG responses were compiled into high-speed video format. Within a single frame corresponding to the period preceding EFS stimulation, manual tracing of all visible cell bodies was performed in ImageJ (NIH, Bethesda, MD). Fluorescent intensity values within each cell region of interest (ROI) over time were exported and analyzed using a custom MATLAB (MathWorks, Natick, MA) script. Briefly, fluorescent signal prior to each EFS stimulation was used to calculate baseline fluorescence within each cell ROI (F_0). This baseline value was used to calculate $\Delta F/F_0$, where ΔF is the rise in fluorescence due to EFS at each stimulation voltage. A piecewise cubic interpolating polynomial was used to correct for drift in baseline fluorescence with time prior to each stimulus using the local minimum (F_0) within each ROI prior to EFS. A peak-detecting algorithm was used to detect calcium responses following each voltage stimulus, and the threshold for a positive response was set to 20% of an individual neuron's maximum $\Delta F/F_0$ peak height.³ This on-off binarization of sensory neuron Ca^{2+} signaling, when assessed by GCaMP fluorescence, has been previously reported by Hartung and Gold.¹⁶ For each DRG, the percent of responding neurons at each voltage amplitude was calculated by normalizing the number of responding neurons at each

amplitude by the highest number responding across all amplitudes.

Statistical Analysis

All statistical analyses were performed in Prism 8 (GraphPad, San Diego, CA). A repeated measures two-way ANOVA with Bonferroni *post hoc* was used to test for differences in percent responding cells at each voltage between trials in repeatability experiments. A constrained sigmoidal fit was performed on population response data to determine a half-maximal response voltage (EV_{50}) and area under the curve (AUC) was calculated. A paired student *t* test was used to compare EV_{50} and AUC values between trials in reproducibility experiments. Variance data for EV_{50} were used to determine that $n = 13$ DRG tissues would have at least 80% power to detect mean differences of 33% (within-subjects Cohen's $d = 0.85$) based on a two-sided paired student *t* test at a significance level of 0.05. To test for an effect of TTX dose on cellular responses, a repeated measures one-way ANOVA with Dunnett's *post hoc* was used to compare EV_{50} and AUC values at each TTX dose to the 0 μ M untreated control. To investigate the influence of cell size on EFS responsiveness following TTX treatment, neurons were sorted by soma diameter into three groups (diameter < 20 μ m, 20 μ m < diameter < 25 μ m, diameter > 25 μ m) and a repeated measures two-way ANOVA was used to compare EV_{50} values between conditions.¹⁸ All data are presented as mean \pm SD unless otherwise stated, statistical significance was set at $p < 0.05$.

RESULTS

EFS Responses are Reproducible

In DRGs harvested from Advillin-GCaMP6s mice, we identified on average more than 200 individual GCaMP expressing soma within each imaging field (221 ± 64). Following EFS, an increase in GCaMP fluorescence intensity was transiently observed (Fig. 2). Individual cellular responses at each voltage amplitude were well conserved between trials (Fig. 3a), and an average of $84.6 \pm 19.1\%$ of total identified cell soma in DRG responded to EFS during a voltage sweep. Neurons were largely quiescent at EFS amplitudes below 20 V, with only 2.4 and 22.3% of cells responding at EFS voltage amplitudes of 5 and 10 V on average, respectively (Fig. 3b). Within reproducibility validation experiments, there were no detectable differences in percent responsive cells at each voltage in sequential EFS trials (Voltage

$p < 0.0001$, Trial $p = 0.201$, $n = 13$ DRGs with $n \geq 113$ cells per DRG). Based on observed voltage-response behaviors, data were fit with a sigmoidal function on logarithmically transformed voltage amplitudes, and subsequent voltage-response data are presented as linear-log plots. Furthermore, there were no detectable differences between EV_{50} ($p = 0.923$) or AUC ($p = 0.252$) values between individual trials (Figs. 3c and 3d). EV_{50} values were on average 17.2 and 17.1 V in first and second EFS trials, respectively.

Small Molecule Sodium Channel Inhibition Reduces EFS-Induced Signaling

To test for an ability to use the described EFS imaging method as a drug screening platform, DRGs ($n = 5$ with $n \geq 138$ cells per DRG) were treated with the voltage-gated sodium channel inhibitor, TTX. Following TTX treatment, reduced cellular responsiveness led to a rightward shift in the voltage-response curve with increasing concentrations of TTX (Fig. 4a). A dose-dependent increase in EV_{50} was observed with increasing TTX dose ($p < 0.0001$, Fig. 4b). Significantly increased EV_{50} values were observed at 1 ($p = 0.0006$) and 10 μ M ($p < 0.0001$) TTX doses compared to the untreated negative control. Prior to TTX treatment, the average EV_{50} within DRGs was 13.4 V, with TTX treatment these values increased to 51.5 and 60.6 V at 1 and 10 μ M TTX doses, respectively. A corresponding dose-dependent reduction in AUC values were observed with increasing TTX dose ($p < 0.0001$); significant reductions in AUC were observed with 1 ($p = 0.0003$) and 10 μ M ($p < 0.0001$) TTX doses when compared to the untreated negative control (Fig. 4c). TTX-sensitive voltage-gated ion channels are expressed robustly on soma of differing size and sensory-modality; to investigate the effect of TTX inhibition across these neural sub-populations soma were stratified by cellular diameter. Soma size ($p = 0.924$) did not influence EV_{50} values with TTX inhibition ($p = 0.007$) (Figs. 4d and 4e).

DISCUSSION

Here, we describe the development of an *ex vivo* imaging technique for the simultaneous visualization and functional assessment of hundreds of sensory neurons in isolated DRG tissues. By utilizing genetic techniques to drive the robust expression of GCaMP6s in Advillin-expressing neurons, we showed an ability to reproducibly capture voltage-dependent EFS-mediated signaling dynamics; furthermore, we showed an ability to detect pharmacologically-induced alterations to signaling upon voltage-mediated EFS. These results

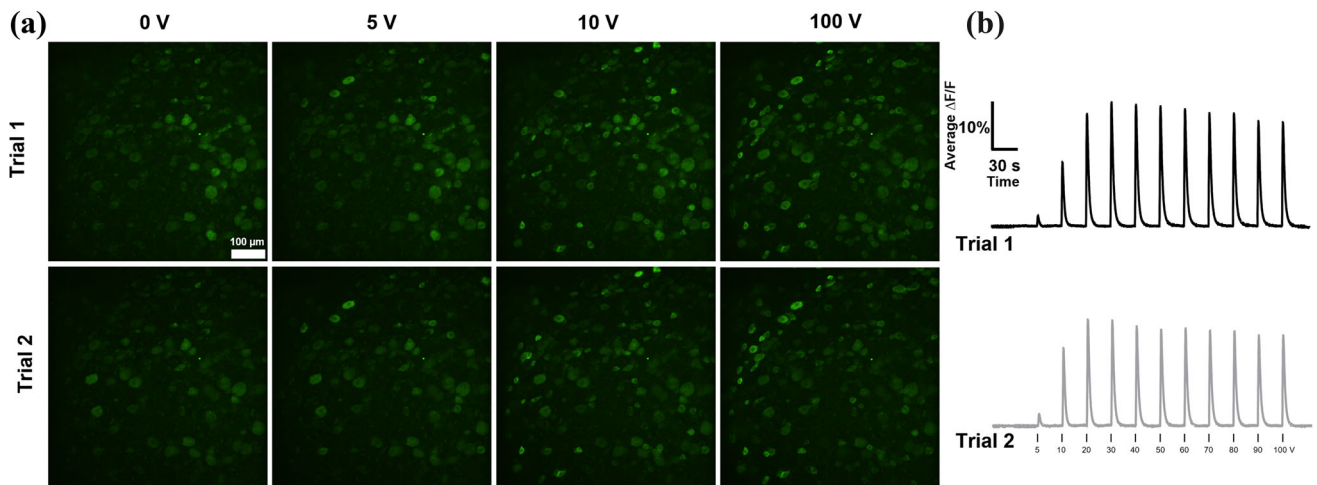


FIGURE 2. Neurons within isolated DRG tissues showed increased GCaMP6s fluorescence (a) shortly following EFS. Average $\Delta F/F$ (b) values across all cellular regions of interest ($n = 286$) within DRG tissues were similar in subsequent trials and generally increased with increasing EFS voltage amplitude. Data from one representative DRG tissue is shown (scale bar = 100 μm).

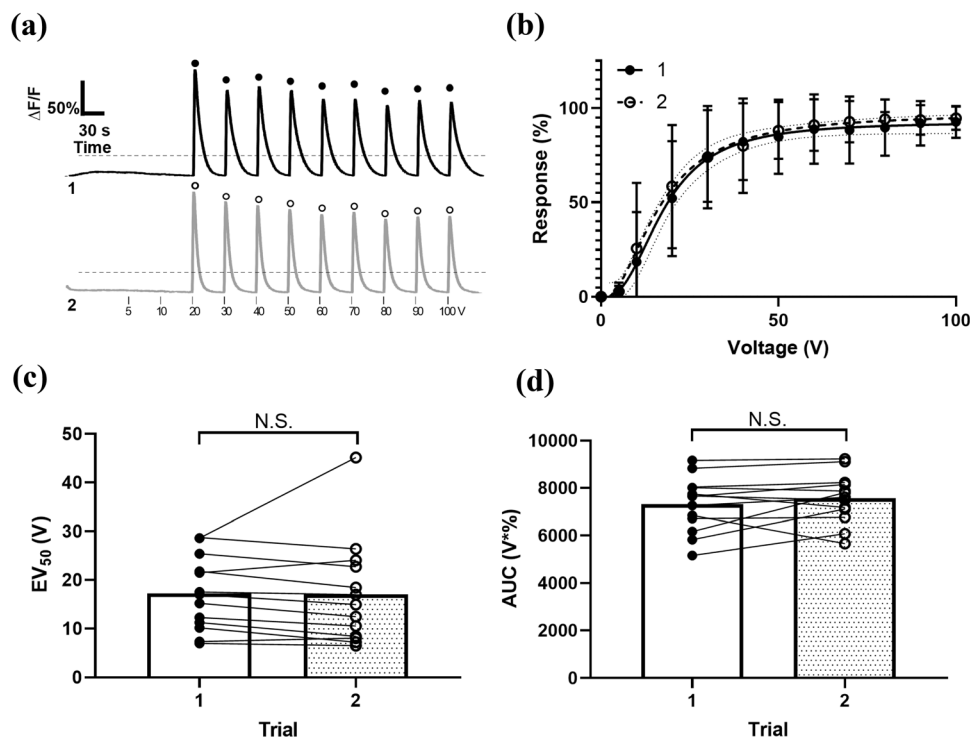


FIGURE 3. (a) Representative traces of an individual neuron in sequential EFS trials, all detected responses are marked by a closed or open circle in the first and second trials, respectively. The dotted line represents the peak height cutoff, which is 20% of the maximum peak height. (b) In subsequent trials, DRG neurons responded similarly to voltage sweeps, and there were no differences in the percent of responding neurons at any voltage (Repeated measures two-way ANOVA; Voltage $p < 0.0001$, Trial $p = 0.201$, mean \pm SD). No significant alterations were observed in EV_{50} ($p = 0.923$) (c) or AUC ($p = 0.252$) (d) values. Repeated measures two-way ANOVA w/Bonferroni's *post hoc* to test for differences between trials at each voltage amplitude, paired student *t* test to test for differences between trials in EV_{50} and AUC ($n = 13$ DRG tissues from 3 mice, with $n \geq 113$ cells per tissue). Sigmoidal fit \pm 95% CI.

highlight the potential utility of the described method which serves as an improved approach for the unbiased and high-throughput *ex vivo* characterization of DRG neuron sensitivity.

Although enzymatic digestion and mechanical dissociation of DRG neurons following axotomy remains the gold standard preparation for *in vitro* experiments of isolated sensory neurons, alterations to cellular

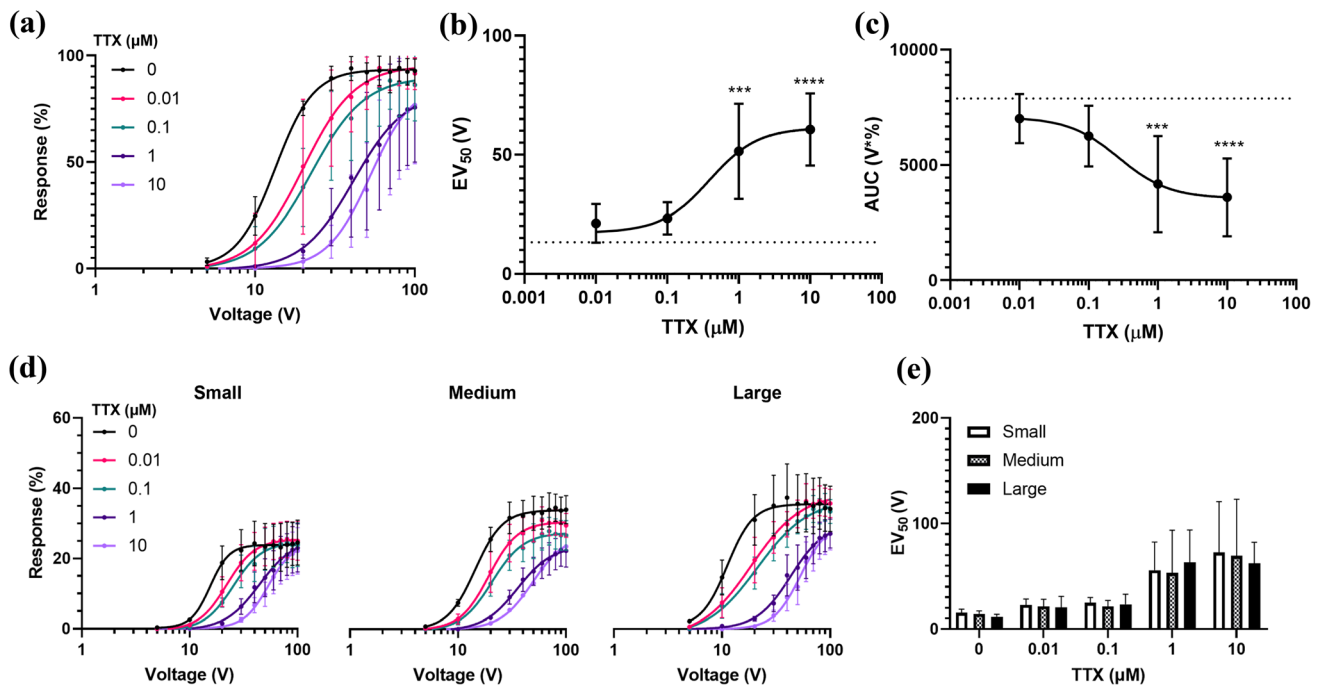


FIGURE 4. TTX inhibits EFS-mediated Ca^{2+} signaling in DRG neurons independent of soma diameter. (a) TTX incubation led to a dose-dependent decrease in EFS mediated cellular response (mean \pm SD). (b) An increase in EV_{50} was observed at 1 ($p = 0.0006$) and 10 μM ($p < 0.0001$) TTX doses while AUC (c) decreased at 1 ($p = 0.0003$) and 10 μM ($p < 0.0001$) TTX doses when compared to untreated controls. (d) Responses in neurons of varying soma size were similar across TTX concentrations. Percent response values in each size group represent a portion of all responding neurons. (e) No size-based differences were observed in EV_{50} at any individual TTX concentration (TTX $p = 0.0007$, Size $p = 0.924$, Repeated measures two-way ANOVA). Repeated measures one-way ANOVA w/Dunnett's *post hoc* was used to test for differences between individual TTX doses and the untreated 0 μM control; *** $p < 0.001$, **** $p < 0.0001$. Dotted line represents 0 μM control, ($n = 5$ DRG tissues from 3 mice, with $n \geq 138$ cells per DRG).

phenotype have been documented in neurons when plated in monolayer culture.^{14,17,31,38} In addition to obvious artifact introduced by cellular dissociation, the spatial organization of individual soma and axons within the DRG are lost with cellular isolation.³⁰ Kim and colleagues have previously shown that with nerve injury, increased calcium signaling occurs in adjacent soma mediated in part through CX43-expressing glial cells, an observation that is lost in dissociated cultures due to disruption of neuron-glial cell interaction.¹⁸ Furthermore, the effects of dissociation may change with time in culture: glial cells have been shown to progressively separate from sensory neuron soma over a 1 week culture period.³⁶ While mitotic inhibitors or growth factors are often required to prevent over-proliferation of satellite cells and improve viability in sensory neurons, respectively, these factors may further contribute to a shift in cell population with time in prolonged monolayer culture.^{28,29,32,33,36}

Prior work has shown EFS can be utilized for the simultaneous and unbiased activation of intracellular Ca^{2+} signaling in large numbers of sensory neurons.^{5,7,8,10,22} Fouillet and colleagues utilized EFS in the development of an *in vitro* drug screening platform

and showed that with increasing doses of TTX, dissociated monolayer cultures of DRG sensory neurons exhibited reduced responses to voltage-mediated stimuli, similar to the results presented in this study.⁸ Others have shown the importance of both high-voltage-gated calcium channels and VGSCs in the generation of EFS mediated Ca^{2+} influx.⁶ Similar work has utilized micro-electrode arrays for the *in vitro* assessment of various pharmacologic modulators of neuronal activity measuring Ca^{2+} mobilization in response to voltage stimuli.²⁷ We believe, however, the method shown in the current study may provide some advantages over these techniques for its abilities to simultaneously assess firing rates in hundreds of cells while maintaining tissue integrity and single-cell firing resolution without the need for more specialized, less readily available, imaging systems such as multi-photon or miniaturized microscopes.^{4,11} Furthermore, the described method does not require exogenous dye loading and instead relies on Cre-driven expression which reduces EFS experimental prep-times and ensures robust and cell-type-specific Ca^{2+} indicator expression. This is in contrast to exogenous dye loading which relies on non-specific diffusion-based cellular

uptake, which may preferentially load satellite glial cells, or micro-pipette injection.^{10,12} Although others have successfully recorded DRG Ca^{2+} transients *en bloc* using single point laser-scanning microscopy, such techniques have been unable to consistently image more than 100 soma per field of view at high frame-rates.^{4,7} Alternative confocal imaging methods, as reported here and elsewhere, help to increase the number of soma which can be simultaneously assessed by nearly two-fold, an improvement that serves to enhance the robustness of acquired Ca^{2+} imaging datasets.⁵

Despite the aforementioned benefits this method has over standard protocols to dissociate single neurons from DRG tissues, *en bloc* DRG isolation still requires axotomy, and as a result alterations to neuron excitability using this method are representative of somatic changes. While alterations within the soma are linked to changes at the site of peripheral sensory innervation, this method as described does not allow for the direct interrogation of fully intact sensory units and thus is a limitation of this *ex vivo* approach.²⁶ A further concern is that the electrical impedance of the isolated DRG may result in a heterogeneous electric field across the tissue. These differences, however, are expected to have little effect given the dimensions of individual cells in proportion to the DRG tissue. Additionally, observations in this study were consistent across neurons within DRG of varying size and across trials within the same DRG.

In conclusion, these data demonstrate an ability to use EFS in isolated DRG tissues to simultaneously study the functional signaling dynamics in hundreds of neurons with single-cell resolution. Using the genetically encoded calcium indicator GCaMP6s with standard spinning-disk confocal microscopy, we were able to assess alterations to EFS-induced population responses of DRG neurons following pharmacologic modulation. Taken together, these results suggest the described imaging approach possesses the sensitivity required for the functional assessment of DRG neuron excitability *ex vivo*.

ACKNOWLEDGMENTS

We would like to acknowledge Remy Walk for assisting with animal handling and Sarah Hall for assisting with image analysis.

FUNDING

This study was supported by the NSF DGE-1745038, OREF resident research grant P20-03413, and NIH grants AR070975, AR069588, AR074441, AR077678.

AUTHOR CONTRIBUTIONS

IMB, TMM, MGG, SYT, YQC, and LAS Designed research; IMB, TMM, CG, MNB, JJS, and MCG Performed research; IMB, TMM, MGG, and CG Analyzed data; IMB, TMM, MNB, MGG, and LAS Wrote the paper.

CONFLICT OF INTEREST

The authors report no conflict of interest.

REFERENCES

- ¹Anderson, M., Q. Zheng, and X. Dong. Investigation of pain mechanisms by calcium imaging approaches. *Neurosci. Bull.* 34:194–199, 2018.
- ²Black, B. J., R. Atmaramani, S. Plagens, Z. T. Campbell, G. Dussor, T. J. Price, and J. J. Pancrazio. Emerging neurotechnology for antinociceptive mechanisms and therapeutics discovery. *Biosens. Bioelectron.* 126:679–689, 2019.
- ³Chen, T.-W., T. J. Wardill, Y. Sun, S. R. Pulver, S. L. Renninger, A. Baohuan, E. R. Schreier, R. A. Kerr, M. B. Orger, V. Jayaraman, L. L. Looger, K. Svoboda, and D. S. Kim. Ultrasensitive fluorescent proteins for imaging neuronal activity. *Nature* 499:295–300, 2013.
- ⁴Chen, C., J. Zhang, L. Sun, Y. Zhang, W.-B. Gan, P. Tang, and G. Yang. Long-term imaging of dorsal root ganglia in awake behaving mice. *Nat. Commun.* 10:3087, 2019.
- ⁵Chisholm, K. I., N. Khovanov, D. M. Lopes, F. La Russa, and S. B. McMahon. Large scale *in vivo* recording of sensory neuron activity with GCaMP6. *eNeuro* 5:EN-EURO.0417-17.2018, 2018.
- ⁶Duflo, F., Y. Zhang, and J. C. Eisenach. Electrical field stimulation to study inhibitory mechanisms in individual sensory neurons in culture. *Anesthesiology* 100:740–743, 2004.
- ⁷Emery, E. C., A. P. Luiz, S. Sikandar, R. Magnúsdóttir, X. Dong, and J. N. Wood. In vivo characterization of distinct modality-specific subsets of somatosensory neurons using GCaMP. *Sci. Adv.* 2:1–8, 2016.
- ⁸Fouillet, A., J. F. Watson, A. D. Piekarz, X. Huang, B. Li, B. Priest, E. Nisenbaum, E. Sher, and D. Ursu. Characterisation of Nav1.7 functional expression in rat dorsal root ganglia neurons by using an electrical field stimulation assay. *Mol. Pain* 13:1–13, 2017.

- ⁹Gandini, M. A., A. Sandoval, and R. Felix. Whole-cell patch-clamp recordings of Ca^{2+} currents from isolated neonatal mouse dorsal root ganglion (DRG) neurons. *Cold Spring Harb. Protoc.* 389–395:2014, 2014.
- ¹⁰Gemes, G., A. Koopmeiners, M. Rigaud, P. Lirk, D. Sapunar, M. L. Bangaru, D. Vilceanu, S. R. Garrison, M. Ljubkovic, S. J. Mueller, C. L. Stucky, and Q. H. Hogan. Failure of action potential propagation in sensory neurons: mechanisms and loss of afferent filtering in C-type units after painful nerve injury. *J. Physiol.* 591:1111–1131, 2013.
- ¹¹Ghosh, K. K., L. D. Burns, E. D. Cocker, A. Nimmerjahn, Y. Ziv, A. El Gamal, and M. J. Schnitzer. Miniaturized integration of a fluorescence microscope. *Nat. Methods* 8:871–878, 2011.
- ¹²Grienberger, C., and A. Konnerth. Imaging calcium in neurons. *Neuron* 73:862–885, 2012.
- ¹³Gryniewicz, G., M. Poenie, and R. Y. Tsien. A new generation of Ca^{2+} indicators with greatly improved fluorescence properties. *J. Biol. Chem.* 260:3440–3450, 1985.
- ¹⁴Guan, W., M. A. Puthenveedu, and M. L. Condit. Sensory neuron subtypes have unique substratum preference and receptor expression before target innervation. *J. Neurosci.* 23:1781–1791, 2003.
- ¹⁵Gutruf, P., C. H. Good, and J. A. Rogers. Perspective: implantable optical systems for neuroscience research in behaving animal models—current approaches and future directions. *APL Photonics* 3:120901, 2018.
- ¹⁶Hartung, J. E., and M. S. Gold. GCaMP as an indirect measure of electrical activity in rat trigeminal ganglion neurons. *Cell Calcium* 89:102225, 2020.
- ¹⁷Kaiser, O., P. Aliuos, K. Wissel, T. Lenarz, D. Werner, G. Reuter, A. Kral, and A. Warnecke. Dissociated neurons and glial cells derived from rat inferior colliculi after digestion with papain. *PLoS One* 8:1–14, 2013.
- ¹⁸Kim, Y. S., M. Anderson, K. Park, Q. Zheng, A. Agarwal, C. Gong, Sajilafu, L. A. Young, S. He, P. C. LaVinka, F. Zhou, D. Bergles, M. Hanani, Y. Guan, D. C. Spray, and X. Dong. Coupled activation of primary sensory neurons contributes to chronic pain. *Neuron* 91:1085–1096, 2016.
- ¹⁹Koopmeiners, A. S., S. Mueller, J. Kramer, and Q. H. Hogan. Effect of electrical field stimulation on dorsal root ganglion neuronal function. *Neuromodulation* 16:304–311, 2013.
- ²⁰Lau, J., M. S. Minett, J. Zhao, U. Dennehy, F. Wang, J. N. Wood, and Y. D. Bogdanov. Temporal control of gene deletion in sensory ganglia using a tamoxifen-inducible Advillin-Cre-ERT2 recombinase mouse. *Mol. Pain* 7:100, 2011.
- ²¹Lin, M. Z., and M. J. Schnitzer. Genetically encoded indicators of neuronal activity. *Nat. Neurosci.* 19:1142–1153, 2016.
- ²²Ma, W., Y. Zhang, C. Bantel, and J. C. Eisenach. Medium and large injured dorsal root ganglion cells increase TRPV-1, accompanied by increased $\alpha 2\text{C}$ -adrenoceptor co-expression and functional inhibition by clonidine. *Pain* 113:386–394, 2005.
- ²³MacGregor, D. G., M. Chesler, and M. E. Rice. HEPES prevents edema in rat brain slices. *Neurosci. Lett.* 303:141–144, 2001.
- ²⁴Miller, R. E., Y. S. Kim, P. B. Tran, S. Ishihara, X. Dong, R. J. Miller, and A.-M. Malfait. Visualization of peripheral neuron sensitization in a surgical mouse model of osteoarthritis by in vivo calcium imaging. *Arthritis Rheumatol.* 70:88–97, 2018.
- ²⁵Narahashi, T., J. W. Moore, and W. R. Scott. Tetrodotoxin blockage of sodium conductance increase in lobster giant axons. *J. Gen. Physiol.* 47:965–974, 1964.
- ²⁶Navarro, X., M. Vivó, and A. Valero-Cabré. Neural plasticity after peripheral nerve injury and regeneration. *Prog. Neurobiol.* 82:163–201, 2007.
- ²⁷Novellino, A., B. Scelfo, T. Palosaari, A. Price, T. Sobanski, T. J. Shafer, A. F. M. Johnstone, G. W. Gross, A. Gramowski, O. Schroeder, K. Jügel, M. Chiappalone, F. Benfenati, S. Martinoia, M. T. Tedesco, E. Defranchi, P. D'Angelo, and M. Whelan. Development of micro-electrode array based tests for neurotoxicity: assessment of interlaboratory reproducibility with neuroactive chemicals. *Front. Neuroeng.* 4:4, 2011.
- ²⁸Price, T. J., M. D. Louria, D. Candelario-Soto, G. O. Dussor, N. A. Jeske, A. M. Patwardhan, A. Diogenes, A. A. Trott, K. M. Hargreaves, and C. M. Flores. Treatment of trigeminal ganglion neurons *in vitro* with NGF, GDNF or BDNF: effects on neuronal survival, neurochemical properties and TRPV1-mediated neuropeptide secretion. *BMC Neurosci.* 6:4, 2005.
- ²⁹Shu, X., and L. M. Mendell. Nerve growth factor acutely sensitizes the response of adult rat sensory neurons to capsaicin. *Neurosci. Lett.* 274:159–162, 1999.
- ³⁰Sperry, Z. J., R. D. Graham, N. Peck-Dimit, S. F. Lempka, and T. M. Bruns. Spatial models of cell distribution in human lumbar dorsal root ganglia. *J. Comp. Neurol.* 528:1644–1659, 2020.
- ³¹Takeda, M., M. Takahashi, and S. Matsumoto. Contribution of the activation of satellite glia in sensory ganglia to pathological pain. *Neurosci. Biobehav. Rev.* 33:784–792, 2009.
- ³²Tanner, K. D., J. D. Levine, and K. S. Topp. Microtubule disorientation and axonal swelling in unmyelinated sensory axons during vincristine-induced painful neuropathy in rat. *J. Comput. Neurol.* 395:481–492, 1998.
- ³³Tanner, K. D., D. B. Reichling, and J. D. Levine. Nociceptor hyper-responsiveness during vincristine-induced painful peripheral neuropathy in the rat. *J. Neurosci.* 18:6480–6491, 1998.
- ³⁴Trevathan, J. K., A. J. Asp, E. N. Nicolai, J. Trevathan, N. A. Kremer, T. D. Y. Kozai, D. Cheng, M. Schachter, J. J. Nassi, S. L. Otte, J. G. Parker, J. L. Lujan, and K. Ludwig. Calcium imaging in freely-moving mice during electrical stimulation of deep brain structures. *J. Neural Eng.* 2020. <https://doi.org/10.1088/1741-2552/abb7a4>.
- ³⁵Trevathan, J. K., I. W. Baumgart, E. N. Nicolai, B. A. Gosink, A. J. Asp, M. L. Settell, S. R. Polacinda, K. D. Malerick, S. K. Brodnick, W. Zeng, B. E. Knudsen, A. L. McConico, Z. Sanger, J. H. Lee, J. M. Aho, A. J. Suminski, E. K. Ross, J. L. Lujan, D. J. Weber, J. C. Williams, M. Franke, K. A. Ludwig, and A. J. Shoffstall. An injectable neural stimulation electrode made from an in-body curing polymer/metal composite. *Adv. Healthc. Mater.* 8:1900892, 2019.
- ³⁶Valtcheva, M. V., B. A. Copits, S. Davidson, T. D. Sheahan, M. Y. Pullen, J. G. McCall, K. Dikranian, and R. W. Gereau. Surgical extraction of human dorsal root ganglia

- from organ donors and preparation of primary sensory neuron cultures. *Nat. Protoc.* 11:1877–1888, 2016.
- ³⁷Verkhatsky, A., O. A. Krishtal, and O. H. Petersen. From Galvani to patch clamp: the development of electrophysiology. *Pflugers Arch. Eur. J. Physiol.* 453:233–247, 2006.
- ³⁸Zhang, X., Y. Chen, C. Wang, and L. Y. M. Huang. Neuronal somatic ATP release triggers neuron-satellite glial cell communication in dorsal root ganglia. *Proc. Natl. Acad. Sci. U.S.A.* 104:9864–9869, 2007.

- ³⁹Zhu, J., G. Zhen, S. An, X. Wang, M. Wan, Y. Li, Z. Chen, Y. Guan, X. Dong, Y. Hu, and X. Cao. Aberrant subchondral osteoblastic metabolism modifies Nav1.8 for osteoarthritis. *Elife* 9:e57656, 2020.

Publisher's Note Springer Nature remains neutral with regard to jurisdictional claims in published maps and institutional affiliations.